Modulation of the Band Gap Increase in Nanocrystals by Surface Passivation

ARTICLE *in* THE JOURNAL OF PHYSICAL CHEMISTRY C · JUNE 2014

Impact Factor: 4.77 · DOI: 10.1021/jp503701k

THE JOURNAL OF PHYSICAL CHEMISTRY C

Article

pubs.acs.org/JPCC

Modulation of the Band Gap Increase in Nanocrystals by Surface Passivation

Xin Liu,*[,†] Y. Y. Sun,*[,‡] D. West,[‡] Xingfa Gao,[#] and S. B. Zhang*[,‡]

[†]School of Chemistry, Dalian University of Technology, Dalian, Liaoning 116024, China

[‡]Department of Physics, Applied Physics, and Astronomy, Rensselaer Polytechnic Institute, Troy, New York 12180, United States

[#]CAS Key Laboratory for Biomedical Effects of Nanomaterials and Nanosafety, Institute of High Energy Physics, Chinese Academy of Sciences, Beijing 100049, China

ABSTRACT: Quantum size effect (QSE) is of central importance in nanoscience. For semiconductors, it is generally perceived that the QSE raises the band gap of a nanocrystal by effectively increasing the kinetic energies of electrons and holes. Using first-principles calculations and Si nanofilms as a test case, we investigated the impact of surface passivation of nanocrystals on the QSE and extended the view of the traditional QSE, as depicted in the classic effective mass model, to include the quantum boundary effect. We showed that the band gap of Si nanofilms is critically affected by the passivation species at the surface, which could result in not only the commonly observed increase in band gap but also a decrease with respect to the bulk value. The Si nanofilms can have a band gap that is virtually the same as that of bulk Si when film thickness is less than 2 nm. The new understanding of the QSE opens a new degree of freedom in engineering the electronic and optoelectronic properties of nanomaterials.

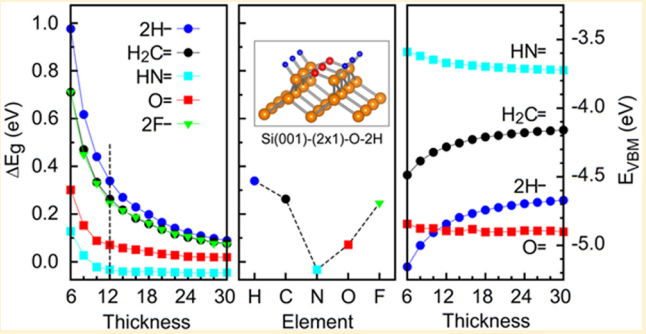

1. INTRODUCTION

Nanomaterials, such as quantum dots, nanowires, and nanofilms, exhibit electronic, optical, and chemical properties that are distinctly different from those of their parent bulk materials. These differences are usually ascribed to quantum size effect (QSE) originating from the confinement of quantum states in the nanomaterials.[1,2] The QSE has opened a myriad of opportunities for many novel applications, such as nanoelectronics, optoelectronics, and photovoltaics.[3,4] One of the major consequences of the QSE is that the band gap of a semiconductor usually increases as its characteristic size is reduced into the nanoregime. The increase in band gap provides a means to tune the optical properties of the nanomaterials,[5] which finds immediate applications in, e.g., light-emitting devices.[6,7] On the other hand, because of the gap increase, electronic screening becomes less effective and impurity states are more localized. Subsequently, the intentional doping of charge carriers in nanocrystals becomes increasingly difficult as the size of the crystals decreases.[8−12] Therefore, instead of accepting the band gap increase as a mandatory consequence of the QSE, it is also of great interest to suppress the QSE when it becomes necessary.

To better control and tune the properties of nanomaterials, it is essential to understand the factors that govern the QSE. The quantum confinements result from the boundaries of nanomaterials, such as the surfaces or the interfaces with matrix materials. The relation between the surface or interface structure and the properties of the nanomaterials is, therefore, of particular importance but has attracted only limited theoretical studies to date.[13,14] The quantum confinement effect is traditionally depicted in the effective mass (EM) particle-in-a-box model,[15] where the quantum confinement on bulk electronic states quantizes the allowed crystal momentum $\mathbf{k}$ in a nanocrystal. Because the $\mathbf{k} = 0$ states, to which the bulk band edge states usually belong, are forbidden in the EM model, gap increase is inevitable.

The EM model, however, does not contain the atomistic details of nanocrystals; therefore, the understanding of the QSE based on the EM model is incomplete. For instance, using a truncated crystal (TC) model, which treats the wave function of a nanocrystal as a linear combination of the periodic Bloch functions, it has been predicted that the reduction in size may not necessarily affect the energy position of the valence band maximum (VBM) state.[16] In other words, the VBM state could be a zero confinement state (ZCS). This result suggests that the band gap increase in nanocrystals could be mainly due to an effect associated with the atomistic details at the boundaries, which are not included in the TC model.

Using first-principles calculations we showed that the QSE on a semiconductor nanocrystal is not a well-defined physical effect without knowing the chemistry and atomic structure at the boundary of the nanocrystal. We extended the view on the

Received: April 15, 2014
Revised: June 1, 2014
Published: June 5, 2014

   dx.doi.org/10.1021/jp503701k | J. Phys. Chem. C 2014, 118, 14026−14030

traditional QSE, as depicted in the classic EM model, to include the quantum boundary effect. Specifically, using silicon (001) nanofilms as an example, we found a strong dependence of the band gap on the choice of surface passivation. For example, for a 1.6 nm thick film, the change in band gap with respect to that of bulk Si can vary between about +55% and −7% when the surfaces are passivated differently. The large variation is mainly determined by how the bulk VBM state interacts with the atomic orbitals associated with the passivation species at the surfaces, which can completely offset the QSE on the band gap.

2. THEORETICAL METHODS

Our first-principles calculations were based on the density functional theory (DFT) within the generalized gradient approximation for the exchange correlation functional.[17] Core electrons were described by the projector augmented wave method as implemented in the Vienna ab initio simulation package (VASP).[18,19] Plane waves with a kinetic energy cutoff of 25 Ry were used as the basis set. The Si(001) nanofilms were modeled by supercells containing periodic slabs with (2 × 1) surfaces and vacuum regions (about 10 Å) separating the slabs in adjacent cells. The optimized lattice constant of Si, 5.468 Å, was used to set up the supercell. The Brillouin zone was sampled by (3 × 5 × 1) Monkhorst−Pack k-point grids.[20] Symmetric slabs with two identical surfaces were adopted in our calculation so that dipole potential is avoided in both the vacuum and bulk regions. Atomic structures were relaxed by minimizing forces on all atoms to within 0.001 Ry/bohr. Calculations with 50 Ry plane-wave cutoff, (5 × 9 × 1) k-point grids, and 15 Å thick vacuum region were carried out to ensure well-converged results.

3. RESULTS AND DISCUSSION

Figure 1a shows the calculated the band gap change ΔE_g with respect to bulk Si (0.6 eV from our DFT calculation) as a function of film thickness N, which represents the number of atomic layers in the film. We started from the canted Si(001)-(1 × 1)-2H surface on each side of the films, denoted as 2H− hereafter.[21] To compare different passivations on the same footing, we used a (2 × 1) surface, i.e., four H atoms per surface cell. Then, we replaced two of the four H atoms by different passivation species, namely, H_2C=, HN=, O=, or 2F−. As an illustration, one of these surfaces (O=) is shown in the inset of Figure 1b. We have verified that these passivations remove all surface states from the band gap, as evidenced by the calculated band structures in Figure 2 for the 2H− and O= films.[22] To illustrate the systematic dependence of E_g on passivation, Figure 1b focuses on the results for N = 12 (corresponding to a nominal film thickness of about 1.64 nm), which shows clearly a large variation.

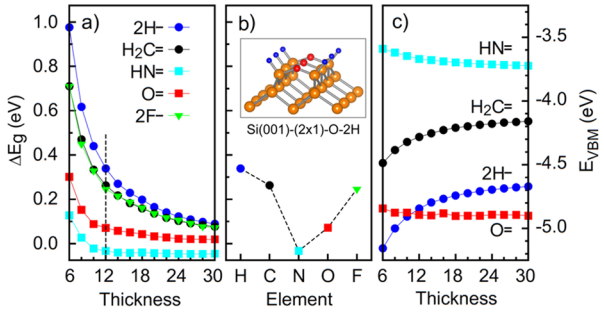

Figure 1. Effects of surface passivation on the electronic structure of Si(001) nanofilms. (a) Band gap change ΔE_g with respect to bulk Si as a function of film thickness (i.e., the number of atomic layers N in the films). (b) ΔE_g at N = 12, corresponding to the dashed line in panel a. (c) VBM energy E_{VBM} with respect to the vacuum level as a function of N.

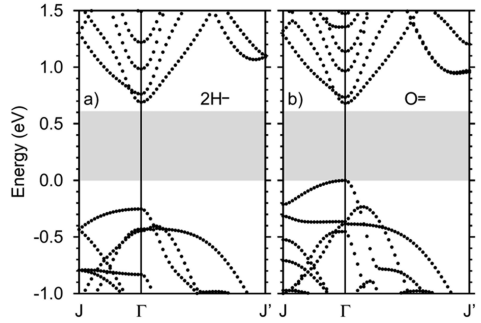

Figure 2. Band structures of 12-layer-thick Si(001)-(2 × 1) films with (a) 2H− and (b) O= passivation. The gray regions show the band gap of bulk Si. The Γ point denotes the center of the Brillouin zone. Γ−J and Γ−J' correspond to the 2× and 1× directions, respectively, of the (2 × 1) surface cell.

To discuss the results above, it is beneficial to introduce the results from the TC model,[16] which offers an improved understanding of the QSE by taking into account atomistic details of the nanocrystal. One result from the TC model that is qualitatively different from the EM model is that, in addition to the standard particle-in-a-box confinement states as exemplified in Figure 3a, there also exist anticonfinement states, whose envelope functions have a significant magnitude at the

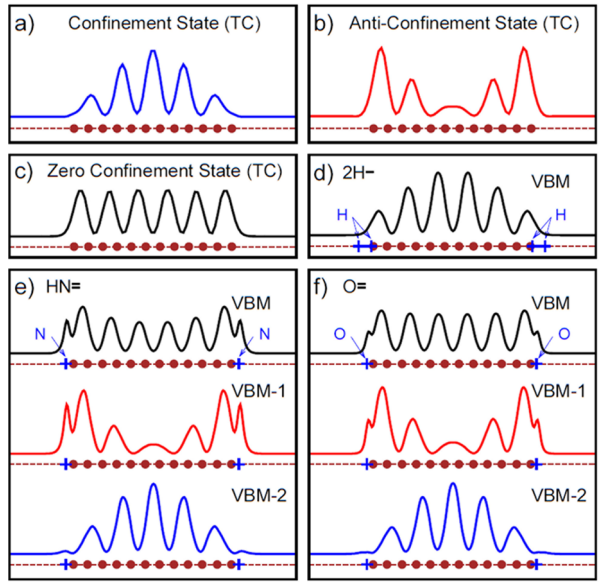

Figure 3. Plane-averaged charge densities (in arbitrary unit) for (a) a confinement state, (b) an anticonfinement state, and (c) the zero-confinement state obtained by TC model calculation (ref 21). (d) VBM state for the 2H− film. Panels e and f show VBM state and adjacent states for the HN= and O= films, respectively. The positions of the Si atomic layers are marked by solid dots. The positions of passivation species are marked by crosses. Panels d−f are obtained by DFT calculation. All states are taken from the center of the surface Brillouin zone (i.e., the Γ point).

dx.doi.org/10.1021/jp503701k | J. Phys. Chem. C 2014, 118, 14026−14030

boundaries. Figure 3b shows an example of the anticonfinement state. The existence of the anticonfinement states is a straightforward way to satisfy the charge neutrality by complementing the confinement states. Because the magnitude of the anticonfinement state is significant (or maximized) at the boundaries (i.e., surfaces), they are more sensitive to the details of boundary conditions, such as surface passivation, as reflected in Figure 1a and discussed below. Another important result of the TC model is that the state at the VBM can be unchanged compared with that in the bulk, which leads to the prediction of zero-confinement state (ZCS) in nanomaterials. Figure 3c shows the ZCS (i.e., the VBM state) from the TC model calculation for the case with N = 12. The ZCS can be considered as a special case of anticonfinement state in the sense that its envelope function also has significant magnitude at the boundary. Therefore, the ZCS is expected to be sensitive to the surface passivation, too.

To gain more physical insights, we make a comparison of our first-principles results with the predictions of the TC model. Figure 3 shows the plane-averaged charge densities calculated using the TC model (Figure 3a–c) and DFT calculations for the 2H–, HN═, and O═ films (Figure 3d–f), where N = 12. In Figure 3d–f, the VBM states are all ZCS-derived having six Si-related peaks and a minimum at the center of the slab, the same as the ZCS state shown in Figure 3c. However, the envelop functions of the 2H–, O═, and HN═ films are qualitatively different. One of them (2H–) is well-confined; one (O═) is nearly unconfined (i.e., bulk-like); and the third one (HN═) is anticonfined (i.e., having larger magnitude near the surface than the interior). The results can be correlated to the change in VBM position shown in Figure 1c, which shows a significant downward bending, almost no bending, and slightly upward bending of the E_{VBM} in the cases of 2H–, O═, and HN═ films, respectively.

We also plotted the two states immediately below the VBM for HN═ and O═ in panels e and f of Figure 3, respectively. In the TC model calculation, the confinement and anticonfinement states, as shown in panels a and b of Figure 3, respectively, are the two states below the ZCS in Figure 3c. From these plots, clear one-to-one correspondence between the TC model states and those from the nanofilms with real surface passivation can be seen. The most prominent difference between the TC model and the present results is on the VBM state, as discussed above, which suggests that the band gap change in Figure 1 is determined by the different behavior of the VBM states in the nanofilms with different passivation species.

To understand this, we plotted the charge densities of the VBM states in Figure 4. It can be seen that, in the case of HN═ and O═, the VBM state (of Si p character) couples with the occupied p_z lone-pair state of N and O, respectively. In other words, there exist electronic orbitals in these passivation species that are chemically compatible with the Si VBM state, allowing efficient orbital hybridization. In the case of 2H– and H_2C═, however, there are no such lone-pair states. The incompatibility of these passivation species with the VBM state confines the wave function of the VBM to the internal part of the nanofilm (cf. Figure 3d) resulting in the increase in band gap. In the case where the passivation species is fully compatible with the VBM state (e.g., the HN═ and O═ films are close to such a case), a ZCS occurs and the boundary appears "invisible" to the corresponding quantum mechanical wave. It is worth noting that the passivation-induced surface

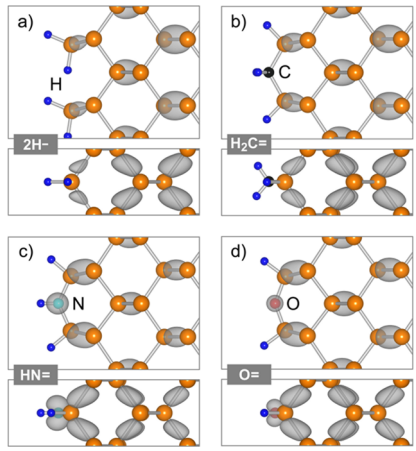

Figure 4. Charge density of the VBM state near the surface for 12 layer thick (a) 2H–, (b) H_2C═, (c) HN═, and (d) O═ Si nanofilms. Two perpendicular {110} planes are shown, one in the 2× and the other in the 1× direction of the (2 × 1) surface.

dipole typically shifts the VBM and CBM by a similar amount[23] and therefore is not expected to account for the QBE discussed above.

Hydrogen, oxygen, and their combinations are the most widely used passivation species for Si. We have studied the thermodynamic stabilities of various O (or N) passivation as a function of the H and O (or N) chemical potentials. We evaluate the passivation energy according to $E_{film} - n_{Si}\mu_{Si} - n_X\mu_X - n_H\mu_H$, where E_{film} is the total energy of a passivated film, n the number of atoms, μ the corresponding chemical potential, and X = N or O. We take μ_{Si} to be the total energy per atom in bulk Si. Figure 5 shows the stability diagram as a function of $\Delta\mu$

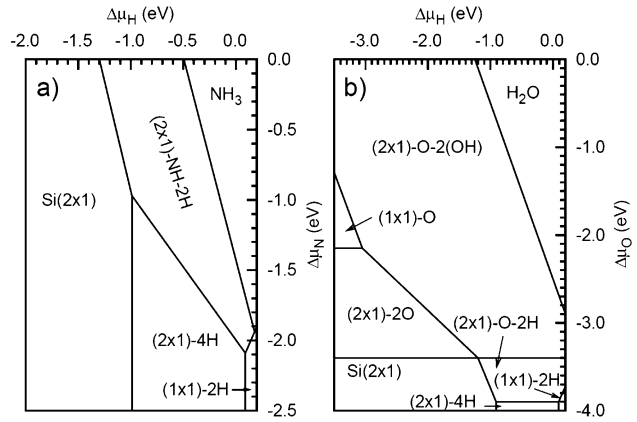

Figure 5. Stability diagram showing the most stable surface structures with N (a) and O (b) passivation as a function of chemical potentials. The presence of H has been considered. The regions labeled NH_3 and H_2O are nonchemisorption regions where NH_3 or H_2O is in the corresponding gas phase. As such, the most accessible $\Delta\mu$ regions are those as large as possible but still outside the NH_3 (or H_2O) region.

of O (or N) and H, where $\Delta\mu$ = 0 is set to be the total energy per atom in N_2, O_2, and H_2 molecules. Using the ideal gas approximation, one can map $\Delta\mu$ to temperature and H_2, O_2, or N_2 gas pressures during growth.[24−26] Figure 5 indicates that the (2 × 1)-O-2(OH), (2 × 1)-O-2H, and (2 × 1)-NH-2H surfaces are the most easily achieved surfaces under normal experimental conditions.[27] Indeed, experiment with H and O copassivation of Si quantum dots has suggested surfaces similar

dx.doi.org/10.1021/jp503701k | J. Phys. Chem. C 2014, 118, 14026−14030

to (2 × 1)-O-2H and (2 × 1)-O-2(OH).[28,29] Thus, the effect proposed here is expected to be observed in experiments with accurate surface structure control.

4. CONCLUSION

In summary, we extended the understanding of the traditional QSE to include the quantum boundary effect. We demonstrated that the band gap increase in nanomaterials is not a necessary consequence of the QSE. Using first-principles calculations and Si(001) nanofilms as an example, we showed that the band gap of a nanocrystal is critically affected by how the bulk VBM state interacts with the atomic orbitals associated with the passivation species at the surfaces. Depending on the chemical compatibility with the passivation species, the VBM state can exhibit a traditional confined envelope function, which will increase the band gap, an unconfined, or even a negatively confined envelope function, which can reduce the band gap. New applications of the quantum boundary effect can be expected. For example, one may fabricate heterojunctions based on the same semiconductor material simply by adjusting the band gap of a thin film with different surface passivation. Finally, we note that the QBE, as originated from the hybridization of the VBM state and the atomic orbitals of the passivation agents, should be generally applicable to other semiconductor materials. The details of the hybridization, however, could depend on various factors, such as the chemical composition, atomic structure, and the symmetry of the VBM states and the atomic orbitals, the examination of which requires more theoretical and experimental studies.

AUTHOR INFORMATION

Corresponding Authors

*E-mail: xliu@dlut.edu.cn.
*E-mail: suny4@rpi.edu.
*E-mail: zhangs9@rpi.edu.

Notes

The authors declare no competing financial interest.

ACKNOWLEDGMENTS

We thank V. Meunier for valuable discussions. Y.Y.S. acknowledges support by U.S. National Science Foundation under Grant DMR-1104994. D.W. and S.B.Z. are supported by U.S. Department of Energy (DOE) under Grant DE-SC0002623. X.L. is supported by NSFC (21373036, 21103015, 21271037, and 11174045), the Fundamental Research Funds for the Central Universities (DUT12LK14 and DUT14LK09), the Key Laboratory of Coastal Zone Environmental Processes YICCAS (201203), and the Key Science and Technology International Co-operation Foundation of Hainan Province, China (KJHZ2014-08). The supercomputer time was provided by National Energy Research Scientific Computing Center (NERSC) under DOE Contract DE-AC02-05CH11231 and the Center for Computational Innovations (CCI) at Rensselaer Polytechnic Institute.

REFERENCES

(1) Ledoux, G.; Gong, J.; Huisken, F.; Guillois, O.; Reynaud, C. Photoluminescence of Size-Separated Silicon Nanocrystals: Confirmation of Quantum Confinement. *Appl. Phys. Lett.* **2002**, *80*, 4834−4836.
(2) Zhao, X. Y.; Wei, C. M.; Yang, L.; Chou, M. Y. Quantum Confinement and Electronic Properties of Silicon Nanowires. *Phys. Rev. Lett.* **2004**, *92*, 236805.
(3) Nozik, A. J. Spectroscopy and Hot Electron Relaxation Dynamics in Semiconductor Quantum Wells and Quantum Dots. *Annu. Rev. Phys. Chem.* **2001**, *52*, 193−231.
(4) Li, Y.; Qian, F.; Xiang, J.; Lieber, C. M. Nanowire Electronic and Optoelectronic Devices. *Mater. Today* **2006**, *9*, 18−27.
(5) Dabbousi, B. O.; Rodriguez-Viejo, J.; Mikulec, F. V.; Heine, J. R.; Mattoussi, H.; Ober, R.; Jensen, K. F.; Bawendi, M. G. (CdSe)ZnS Core−Shell Quantum Dots: Synthesis and Characterization of a Size Series of Highly Luminescent Nanocrystallites. *J. Phys. Chem. B* **1997**, *101*, 9463−9475.
(6) Park, N. M.; Kim, T. S.; Park, S. J. Band Gap Engineering of Amorphous Silicon Quantum Dots for Light-Emitting Diodes. *Appl. Phys. Lett.* **2001**, *78*, 2575−2577.
(7) Sun, Q.; Wang, Y. A.; Li, L. S.; Wang, D. Y.; Zhu, T.; Xu, J.; Yang, C. H.; Li, Y. F. Bright, Multicoloured Light-Emitting Diodes Based on Quantum Dots. *Nat. Photonics* **2007**, *1*, 717−722.
(8) Mikulec, F. V.; Kuno, M.; Bennati, M.; Hall, D. A.; Griffin, R. G.; Bawendi, M. G. Organometallic Synthesis and Spectroscopic Characterization of Manganese-Doped Cdse Nanocrystals. *J. Am. Chem. Soc.* **2000**, *122*, 2532−2540.
(9) Erwin, S. C.; Zu, L. J.; Haftel, M. I.; Efros, A. L.; Kennedy, T. A.; Norris, D. J. Doping Semiconductor Nanocrystals. *Nature (London, U.K.)* **2005**, *436*, 91−94.
(10) Rurali, R. Colloquium: Structural, Electronic, and Transport Properties of Silicon Nanowires. *Rev. Mod. Phys.* **2010**, *82*, 427−449.
(11) Chan, T. L.; Tiago, M. L.; Kaxiras, E.; Chelikowsky, J. R. Size Limits on Doping Phosphorus into Silicon Nanocrystals. *Nano Lett.* **2008**, *8*, 596−600.
(12) Liu, X.; Zhang, S. B.; Ma, X. C.; Jia, J. F.; Xue, Q. K.; Bao, X. H.; Li, W. X. Wavevector-Dependent Quantum-Size Effect in Electron Decay Length at Pb Thin Film Surfaces. *Appl. Phys. Lett.* **2008**, *93*, 093105.
(13) Leu, P. W.; Shan, B.; Cho, K. J. Surface Chemical Control of the Electronic Structure of Silicon Nanowires: Density Functional Calculations. *Phys. Rev. B* **2006**, *73*, 195320.
(14) Nolan, M.; O'Callaghan, S.; Fagas, G.; Greer, J. C.; Frauenheim, T. Silicon Nanowire Band Gap Modification. *Nano Lett.* **2007**, *7*, 34−38.
(15) Burt, M. G. The Justification for Applying the Effective-Mass Approxmation to Microstructures. *J. Phys.: Condens. Matter* **1992**, *4*, 6651−6690.
(16) Zhang, S. B.; Yeh, C. Y.; Zunger, A. Electronic-Structure of Semiconductor Quantum Films. *Phys. Rev. B* **1993**, *48*, 11204−11219.
(17) Perdew, J. P.; Burke, K.; Ernzerhof, M. Generalized Gradient Approximation Made Simple. *Phys. Rev. Lett.* **1996**, *77*, 3865−3868.
(18) Kresse, G.; Joubert, D. From Ultrasoft Pseudopotentials to the Projector Augmented-Wave Method. *Phys. Rev. B* **1999**, *59*, 1758−1775.
(19) Kresse, G.; Furthmuller, J. Efficiency of Ab-Initio Total Energy Calculations for Metals and Semiconductors Using a Plane-Wave Basis Set. *Comput. Mater. Sci.* **1996**, *6*, 15−50.
(20) Monkhorst, H. J.; Pack, J. D. Special Points for Brillouin-Zone Integrations. *Phys. Rev. B* **1976**, *13*, 5188−5192.
(21) Northrup, J. E. Structure of Si(100)H: Dependence on the H-Chemical Potential. *Phys. Rev. B* **1991**, *44*, 1419−1422.
(22) We have also studied the HB= passivation. Similar to other passivations, it can remove the dangling bond states on the Si(001) surface. The empty p orbital of B, however, introduces an empty band in the gap. Therefore, the HB= passivation was not discussed in this paper.
(23) Yang, S.; Prendergast, D.; Neaton, J. B. Tuning Semiconductor Band Edge Energies for Solar Photocatalysis Via Surface Ligand Passivation. *Nano Lett.* **2012**, *12*, 383−388.
(24) Reuter, K.; Scheffler, M. Composition, Structure, and Stability of RuO_2(110) as a Function of Oxygen Pressure. *Phys. Rev. B* **2002**, *65*, 035406.
(25) Wang, L.; Sun, Y. Y.; Lee, K.; West, D.; Chen, Z. F.; Zhao, J. J.; Zhang, S. B. Stability of Graphene Oxide Phases from First-Principles Calculations. *Phys. Rev. B* **2010**, *82*, 161406.

(26) Sun, Y. Y.; et al. Phase Diagram of Graphene Nanoribbons and Band-Gap Bifurcation of Dirac Fermions under Quantum Confinement. *Phys. Rev. B* **2012**, *85*, 195464.
(27) We also calculated the electronic structure for the (2 × 1)-O-2(OH) passivation and found that it is similar to (2 × 1)-O-2H showing nearly zero confinement on the VBM State.
(28) Wolkin, M. V.; Jorne, J.; Fauchet, P. M.; Allan, G.; Delerue, C. Electronic States and Luminescence in Porous Silicon Quantum Dots: The Role of Oxygen. *Phys. Rev. Lett.* **1999**, *82*, 197−200.
(29) Peng, C.; Gao, J.; Wang, S.; Zhang, X.; Zhang, X.; Sun, X. Stability of Hydrogen-Terminated Surfaces of Silicon Nanowires in Aqueous Solutions. *J. Phys. Chem. C* **2011**, *115*, 3866−3871.